THE JOURNAL OF PHYSICAL CHEMISTRY Letters

Letter

pubs.acs.org/JPCL

Rapid Energy Transfer Enabling Control of Emission Polarization in Perylene Bisimide Donor−Acceptor Triads

Christopher Menelaou,[†] Jeroen ter Schiphorst,[‡] Amol M. Kendhale,[‡] Patrick Parkinson,[†] Michael G. Debije,[‡] Albertus P. H. J. Schenning,[‡] and Laura M. Herz*[,†]

[†]Department of Physics, University of Oxford, Clarendon Laboratory, Parks Road, Oxford OX1 3PU, United Kingdom

[‡]Functional Organic Materials and Devices, Department of Chemical Engineering and Chemistry, Eindhoven University of Technology, P.O. Box 513, 5600 MB Eindhoven, The Netherlands

Supporting Information

ABSTRACT: Materials showing rapid intramolecular energy transfer and polarization switching are of interest for both their fundamental photophysics and potential for use in real-world applications. Here, we report two donor−acceptor−donor triad dyes based on perylene-bisimide subunits, with the long axis of the donors arranged either parallel or perpendicular to that of the central acceptor. We observe rapid energy transfer (<2 ps) and effective polarization control in both dye molecules in solution. A distributed-dipole Förster model predicts the excitation energy transfer rate for the linearly arranged triad but severely underestimates it for the orthogonal case. We show that the rapid energy transfer arises from a combination of through-bond coupling and through-space transfer between donor and acceptor units. As they allow energy cascading to an excited state with controllable polarization, these triad dyes show high potential for use in luminescent solar concentrator devices.

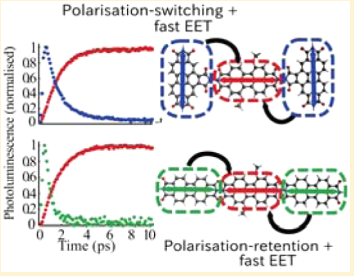

Since the turn of the century, global photovoltaic (PV) capacity has increased on average by 42% each year, from 1.5 GW to 70 GW,[1] yet despite this tremendous growth, renewables still account for a relatively small fraction of total energy production. PV system prices have fallen consistently by 6−8% per year since 1998, but the cost of energy generated from silicon PV is still relatively high.[2] Crystalline silicon PVs are inefficient when operating in low light conditions and when the incident radiation is off normal incidence. Although optical concentrators using mirrors or lenses can reduce the amount of PV material required by focusing a large amount of sunlight onto a small area cell and active tracking mechanisms can be used to ensure continuous energy generation, these components constitute a large portion (approximately 60−70%) of the total device cost[2] but are unable to fully compensate for the reduced PV performance in diffuse light conditions. Therefore, they are unsuitable for use in climates where the weather is often overcast or in urban environments where space is a premium.

Luminescent solar concentrators (LSC)[3−5] are a separate class of concentrator devices based on a luminescent material embedded in a transparent lightguide. Incident light is absorbed and then re-emitted at longer wavelengths, with a large proportion of the re-emitted light carried to the edges of the guide by total internal reflection, where it is coupled out to PV cells distributed around the edges.[6] In general, the intensity of light at the edges relative to that incident on the front surface is much smaller than the surface to edge ratio of the device. There are many loss sources associated with LSC,[7] but three of the major sources are due to incomplete absorption across the solar spectrum by the luminescent material, self-absorption losses during transit from the original absorber to the lightguide edge, and escape from the front surface which is not internally reflected. Attempts to address the first of these issues have been made by using stacks of multiple layers, each absorbing over a different part of the spectrum,[4] or multiple dyes in the same film.[4,8] In order to direct photoluminescence away from the surface, an anisotropic distribution of luminophores is crucial.[9,10] Anisotropic dye distribution results in a larger fraction of the emitted photoluminescence (PL) being directed toward the edges of the lightguide and away from the surface, reducing escape losses,[11,12] while energy transfer between donor and acceptor units on the same molecule reduces self-absorption losses, as we have recently shown.[13] A donor−acceptor−donor triad dye with two unsubstituted perylene bisimide (PBI) donors and one bay-substituted PBI acceptor in a collinear arrangement was incorporated into a switchable LC host. The elongated shape of the triad molecule enabled facile alignment with the LC host, while the 2:1 ratio of donors to acceptors means that self-absorption effects could be minimized without compromising on incident light absorption.

In PBI, the dipole moment of the S1 transition is aligned along the long axis of the perylene unit.[14,15] Thus, when the linear triad dyes are all aligned with the LC host, there is very little absorption of light polarized perpendicular to the long molecular axis. Incorporating a second dye that shows the same efficient intramolecular energy transfer from donor to acceptor units but has orthogonal donor and acceptor S1 transition

Received: January 27, 2015
Accepted: March 12, 2015
Published: March 12, 2015

DOI: 10.1021/acs.jpclett.5b00183
J. Phys. Chem. Lett. 2015, 6, 1170−1176

dipole moments would enable more complete absorption of incident light with any polarization while further lowering self-absorption losses. Such an arrangement, however, would be expected to show very low energy transfer rates from a simple Förster model.

Here, we present such a triad dye, which shows switching of photoluminescence polarization along with exceptionally fast excitation energy transfer (EET), in contrast to predictions of the Förster model. We directly compare the photophysics of the D−A−D triad in which D/A dipole moments are orthogonal with a triad in which the dipole moments are collinear. We observe rapid energy transfer ($\tau \approx 1$ ps) and strong PL anisotropy in both molecules when the donor units are selectively excited. The broad absorption across much of the visible spectrum of these two dyes, along with the efficient energy transfer and PL polarization switching makes these dyes ideally suited to use in LSC devices.

The dyes investigated in this study are based on a central bay-substituted perylene bisimide, directly linked to either two benzoperylene trisimides[16] or two unsubstituted perylene bisimide units. Bay substitution lowers the energy of the S1 ← S0 transition relative to the unsubstituted dye (see **A** as compared to **DL** in Figure 1 and Supporting Information Figure S4), allowing the central unit to act as an acceptor and the outer two units as donors in energy transfer processes and minimizing reabsorption by the donor units of any PL emitted by the acceptor in the LSC. In addition, bay substitution increases solubility and ease with which these and similar dyes can be incorporated into a host matrix, making them promising for use in LSC.[17−19] The molecular structures of the two triads (**TH**, **TL**) are shown in Scheme 1, along with those of the donor and acceptor reference molecules (**DH**, **DL**, **A**). Dyes **TL**, **DH**, **DL**, and **A** were synthesized as previously reported.[13] A description of the synthesis for dye **TH** is included in Supporting Information, along with complete characterization details of all dyes used herein.

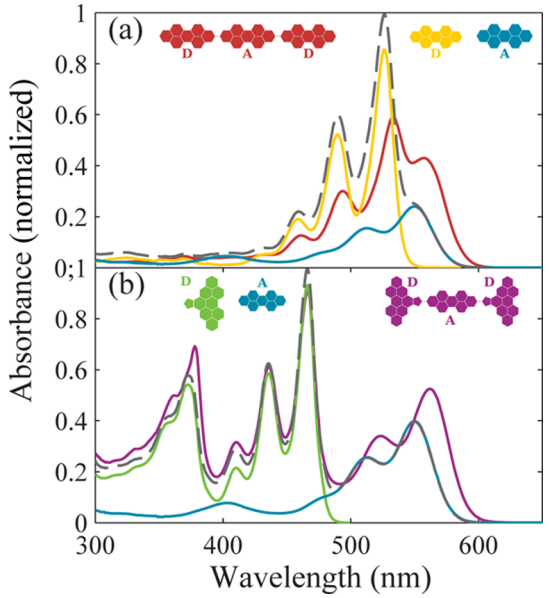

Figure 1. Absorption spectra of (a) dyes **TL**, **DL**, and **A** and (b) dyes **TH**, **DH**, and **A** in $CHCl_3$, normalized to the sum of the donor and acceptor absorbance. Solutions of triad dyes **TH** and **TL** and of **A** had a concentration of 10 μM, whereas **DH** and **DL** were at 20 μM. Spectra were recorded with a PerkinElmer Lambda 1050 spectrophotometer. The solid lines are the experimentally measured data and the dashed gray line in each case is the linear combination of the individual dye and acceptor spectra.

Scheme 1. Chemical Structures of the Five Dyes Used in This Study[a]

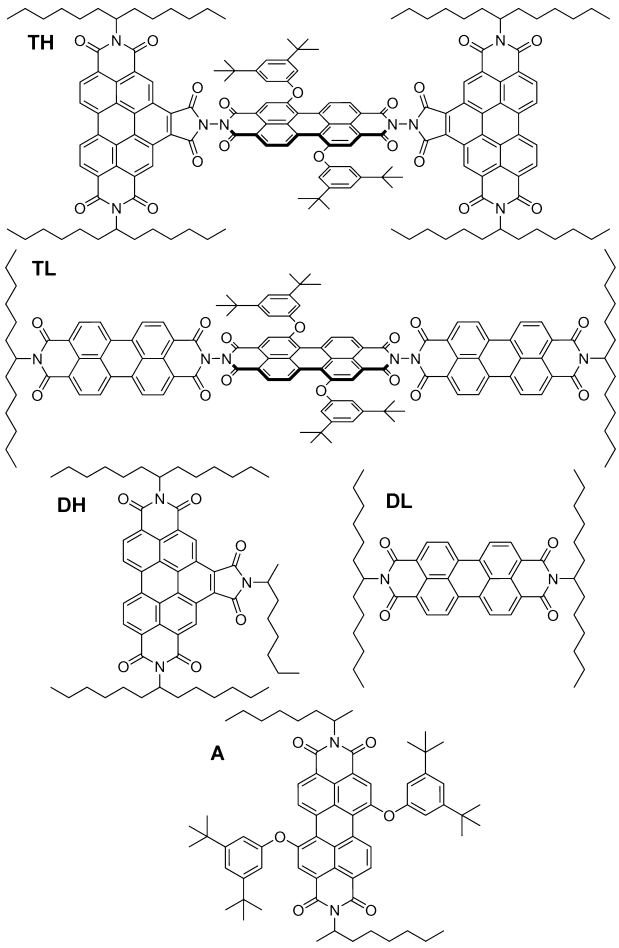

[a]Dyes **TH** and **TL** are the H-shaped and linear donor−acceptor dye triads, dyes **DH** and **DL** are their respective donor moieties, and dye **A** is the acceptor perylene bisimide common to both.

Because for each of the donors and the acceptor, the lowest lying optically active transition has a dipole moment polarized along the long (N−N) axis of the perylene bisimide backbone,[14,15] the dye with benzoperylene donors is referred to as the H-shaped triad (**TH**) due to the orthogonal arrangement of these transition dipoles, whereas the triad with collinear transition moments is referred to as the linear triad (**TL**).

Figure 1 shows the optical absorption spectra of **TH** and **TL** triad dyes in solution. The lowest energy 0−0 peaks located at 465 nm (**TH**, **DH**), 527 nm (**DL**), and 550 nm (**A**) correspond to S1 ← S0 transitions with dipole moment along the long axis of the perylene bisimide unit.[14,15] Higher energy transitions located around 375 nm in **TH** and **DH** have an associated transition dipole moment perpendicular to the PBI long axis and involve the attached benzene and bisimide functional groups of the donor unit.[20]

For these absorption measurements, solutions of the triad dyes and acceptor monomer were prepared at a concentration of 10 μM and those of the donor monomers at 20 μM.

DOI: 10.1021/acs.jpclett.5b00183
J. Phys. Chem. Lett. 2015, 6, 1170−1176

Therefore, the overall concentration of donor and acceptor units was the same in all cases, whether they were part of a triad or free in solution. As a result, the linear sums of the donor and acceptor spectra as shown in Figure 1 by the gray dashed lines would be expected to match the spectra of the triad dyes in the absence of any direct electronic coupling between subunits. In reality, however, a strong degree of coupling between subunits is observed; both donor and acceptor absorption peaks are red-shifted relative to those of the isolated molecules. In particular, the peaks corresponding to S1 ← S0 transitions of the donor and acceptor units in the **TL** are red-shifted by approximately 42.5 and 30.2 meV respectively, compared to the reference molecules **DL** and **A**. In the H-shaped triad **TH**, the donor S2 ← S0 and acceptor S1 ← S0 transitions are red-shifted by 35.6 and 50.8 meV, whereas the donor S1 ← S0 peak remains unchanged. A strong degree of electronic coupling is also evident in the steady-state photoluminescence spectra (see Supporting Information) as the emission peak of the acceptor incorporated into the triads **TL** (**TH**) is red-shifted by 31.2 (42.4) meV relative to the isolated acceptor.

We investigated the rate of energy transfer occurring in the triads by probing both the donor and acceptor emission intensity after selective excitation of the donor subunit. Time- and polarization-resolved photoluminescence spectra and transients were recorded with subpicosecond resolution using the photoluminescence upconversion technique as described in the Supporting Information. Concentrated solutions of dyes **TH** and **TL** were each excited with the frequency doubled output of a Ti:sapphire laser at 450 nm, as there is a minimum in the acceptor unit absorption spectrum at this wavelength, allowing for preferential excitation of the donor subunits (at 450 nm, the total donor absorption is 5.4 and 3.2 times that of the acceptor in dyes **TH** and **TL** respectively, see Figure 1). Figure 2 shows the normalized time-resolved PL spectra for both triads at times ranging from 0.1 to 100 ps after excitation, and the insets show the unscaled PL data. For **TH**, emission from the donor unit centered at 510 nm can be observed immediately after excitation, which rapidly decays while the acceptor emission increases. Even at short times (0.1 ps) after initial excitation there is considerable acceptor emission, which may arise from ultrafast energy transfer or some residual direct acceptor excitation. The red shift of the main acceptor PL peak during and after the decay of the donor emission is assigned to solvent reorientation and relaxation processes.[21] A lowering in energy of the peak emission by 50 meV over the same 100 ps window is also observed in the isolated acceptor in solution (see Figure 2c and Supporting Information). Similar trends are observed for **TL**, although here the donor emission is spectrally not as well resolved as it occurs closer in energy to that of the acceptor unit and, hence, appears as a shoulder on the blue-end of the peak; however, visual inspection suggests that energy transfer is even faster for **TL**.

We are able to determine the rate of excitation energy transfer by following the emission intensity after excitation at a wavelength specific to either the donor or the acceptor. Figure 3a shows the time resolved PL from donor and acceptor units following preferential excitation of the donors at 450 nm. For each of the two triads, rapid quenching of the donor emission is observed, resulting from efficient EET with a rate of $k_1 = 8.3 \times 10^{11}$ s^{-1} (τ_1 = 1.2 ps) for **TH** (a similar transfer rate was reported in related D−A dyad molecules[22]) and a faster rate of $k_2 = 1.6 \times 10^{12}$ s^{-1} (t_2 = 0.6 ps) for **TL**. These values were extracted by fitting the data with a monoexponential decay

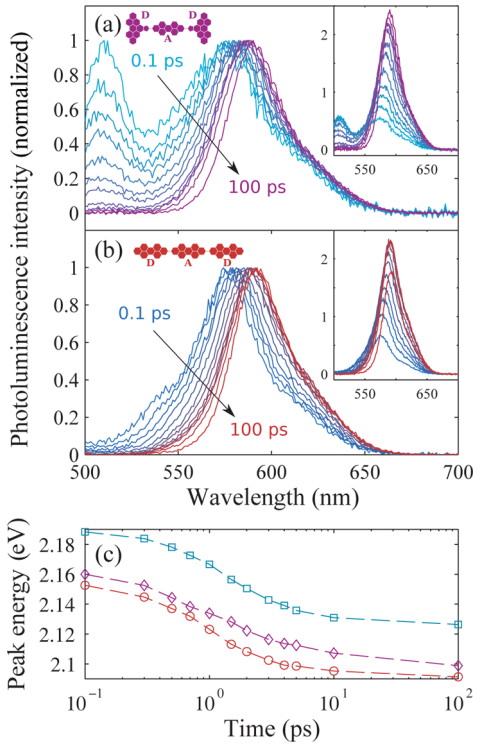

Figure 2. (a,b) The time-resolved PL spectra of dyes **TH** and **TL** at 4 × 10^{-4} M in $CHCl_3$ at short times (0.1 to 100 ps) after excitation. The main plot shows the normalized time-resolved PL, whereas the insets show the raw data. Each spectrum was corrected for the spectral response of the system. (c) Peak emission energy as a function of time after excitation for triad dyes **TH** (diamonds) and **TL** (circles) and for **A** (squares) as a reference. The normalized and raw PL upconversion spectra for **A** are shown in the Supporting Information.

convoluted with the instrument response function taking into account the spatial excitation profile in the cuvette.

To investigate whether such ultrafast energy transfer induces a change in the direction of the oscillator dipole moment, we separately recorded the transients of the emission intensity with polarization parallel ($I_\parallel$) and perpendicular ($I_\perp$) to the polarization of the excitation beam. From these data, the time-dependent PL anisotropy r can be derived as usual, using $r = (I_\parallel - I_\perp)/(I_\parallel + 2I_\perp)$, with the result displayed in Figure 3b. The use of a polarized excitation beam will result in preferential excitation of those molecules with absorption transition moment collinear with the polarization.[23] For a system of randomly oriented molecules with perfectly aligned absorption and emission dipole moments, an initial PL anisotropy of 0.4 is expected as a result.[23,24] However, for a system in which all emission dipole moments are perpendicular to the molecular absorption moments, an anisotropy of −0.2 is to be observed.[23] Hence, for the linear PBI triad **TL**, excitation of solely the donor, followed by complete energy transfer to the acceptor, is expected to yield a value of close to r = 0.4 for perfect alignment of the coupled donor and acceptor dipole moments. On the other hand, a value of r = −0.2 would be associated with a polarization flip by 90° on transfer. However, these values may in reality be modified by the presence of direct acceptor absorption and imperfect dipole alignment.

For the H-shaped triad **TH**, the PL anisotropy of the acceptor emission rapidly falls to a stable value of −0.05, indicating a significant rotation of polarization between absorption and emission dipole moments (Figure 3b). If a

DOI: 10.1021/acs.jpclett.5b00183
J. Phys. Chem. Lett. 2015, 6, 1170−1176

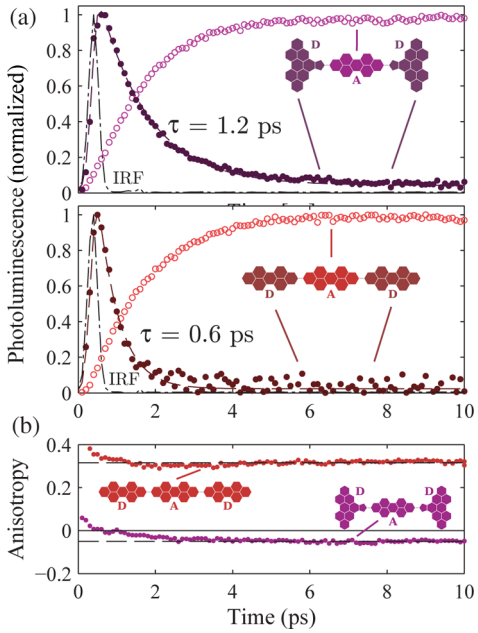

Figure 3. (a) Total PL intensity and (b) PL anisotropy as a function of time after excitation for the triads **TH** and **TL**. In each case, the solid (empty) circles show the PL and anisotropy measured at 510 nm (620 nm). The dashed lines are lifetime fits with a monoexponential decay, convoluted with the instrument response function (dot-dash line). Lifetimes of τ = 1.2 ps and τ = 0.6 ps were determined for **TH** and **TL**, respectively. The point of t = 0 for the PL anisotropy was defined as the time at which the normalized PL intensity was unity. The excitation wavelength for both measurements was 450 nm and the dyes were at a concentration of 4×10^{-4} M in $CHCl_3$.

perfect 90° angle was held between the transition dipoles of the donor and acceptor subunits, we would expect a final anisotropy of −0.10, taking into account the fraction of direct acceptor excitation derived from the relative absorptivity of the subunits at 450 nm. The observed value of −0.05 is higher than this, and would be commensurate with an angle of 72° between dipole moments,[23] suggesting that the long axes of adjacent PBI units in **TH** may not be perfectly perpendicular.

The PL anisotropy of the linear triad **TL** has a starting value of 0.4 at time t = 0, partly influenced by some direct excitation of the acceptor, then decays to a stable value of 0.32 upon EET. These data demonstrate that the emission dipoles of the subunits in this dye are aligned and polarization is mostly retained on EET, although as is the case with **TH**, this alignment appears to be slightly imperfect.

From the perspective of Förster EET theory,[25,26] the ultrafast energy transfer observed for **TH** is highly surprising, given that the transition dipoles for emission/absorption of donor/acceptor units are expected to be fairly orthogonal. In Förster's model, energy transfer is mediated by a Coulombic interaction between transition dipole moments on the donor and acceptors at a rate k, given by

$$k = \frac{9000(\ln 10)\kappa^2 \Phi_D J_{DA}}{128\pi^5 N_A n^4 \tau_D |\mathbf{R}_{DA}|^6} \quad (1)$$

where Φ_D is the fluorescence quantum yield of the donor, τ_D is the radiative lifetime of the donor emission, N_A is Avogadro's constant, n is the refractive index of the medium (n = 1.446 for $CHCl_3$), and $|\mathbf{R}_{DA}|$ is the distance between the donor and acceptor point dipoles associated with the transitions. The orientation factor, κ is given by

$$\kappa = \hat{\mu}_A . \hat{\mu}_D - 3(\hat{\mu}_A . \hat{R}_{DA})(\hat{\mu}_D . \hat{R}_{DA}) \quad (2)$$

where $\hat{\mu}_A$ and $\hat{\mu}_D$ are the unit vectors of the transition dipole moments on the donor and acceptor respectively, and $\hat{\mathbf{R}}_{DA}$ is the unit vector along the line connecting the two. J_{DA} describes the degree of overlap between the normalized donor emission and acceptor extinction coefficient as

$$J_{DA} = \int_0^\infty F_D(\lambda)\varepsilon_A(\lambda)\lambda^4 d\lambda \quad (3)$$

For a system in which the transition dipoles of the donor and acceptor are orthogonal to each other and to the vector connecting them, a value of κ = 0 is obtained, and hence, energy transfer is absent. One key assumption is that the transition dipoles on the two units involved in EET can be modeled as point dipoles; that is, they are small compared to the separation between them. In dyes such as the triads investigated here, this is obviously not the case, as both the length of the perylene bisimides and the separation between them are on the order of 1−2 nm.

To assess whether such electronic wave function delocalization can account for the observed ultrafast energy transfer in **TH**, we compare experimentally extracted rates to a suitably modified version of Förster theory. There are several methods of accounting for the breakdown of the dipole approximation including the line-dipole,[27] distributed-monopole,[28] and transition density cube[29] models. These models are applicable to cases with very weak coupling between chromophores such as **TH**, in which there is no shift of the donor S1 peak positions despite the close proximity of donor and acceptor.[30]

Here, we have used a two-dimensional variation of the line-dipole model that takes into account coupling between local transition densities in the plane of the donor and acceptor molecules. The transition density on the donor and acceptor was approximated as the ground state of a 2-D particle in a box, and split into n_i and n_j subunits μ_i and μ_j as depicted schematically in Figure 4a. A sum over the interaction between each element of the total dipole moments was incorporated into the EET model such that the transfer rate k_{2D} is given by[27,31,32]

$$k_{2D} = \frac{9000(\ln 10)\Phi_D J_{DA}}{128\pi^5 N_A n^4 \tau_D}\left[\sum_{i,j}^{n_i,n_j}\left|\frac{\mu_i \mu_j \kappa_{ij}}{|\mathbf{R}_{ij}|^3}\right|\right]^2 \quad (4)$$

where μ_i and μ_j are the transition dipole moment elements, κ_{ij} is the orientational factor between each subunit as given in eq 2, and $\mathbf{R}_{ij}$ is the distance vector between the midpoints of the interacting elements.

The calculated energy transfer rates are shown in Figure 4b for **TH** (top) and **TL** (bottom). The energy transfer rate (k_{FRET}) as a function of the number of elements along the long axis of the donor and acceptor units (n_i) are plotted for each with dashed lines included as a guide to the eye. For a value of n_i = 1, eq 4 reduces to the simple Förster model; here, an energy transfer of identically zero is obtained for dye **TH** assuming orthogonal transition dipole moments. For any number of elements n_i > 1, however, rapid energy transfer on the order of $(26\ \text{ps})^{-1}$ for **TH** and $(0.15\ \text{ps})^{-1}$ for **TL** are predicted, highlighting the importance of taking the spatial extent of the transition dipoles into account.

DOI: 10.1021/acs.jpclett.5b00183
J. Phys. Chem. Lett. 2015, 6, 1170−1176

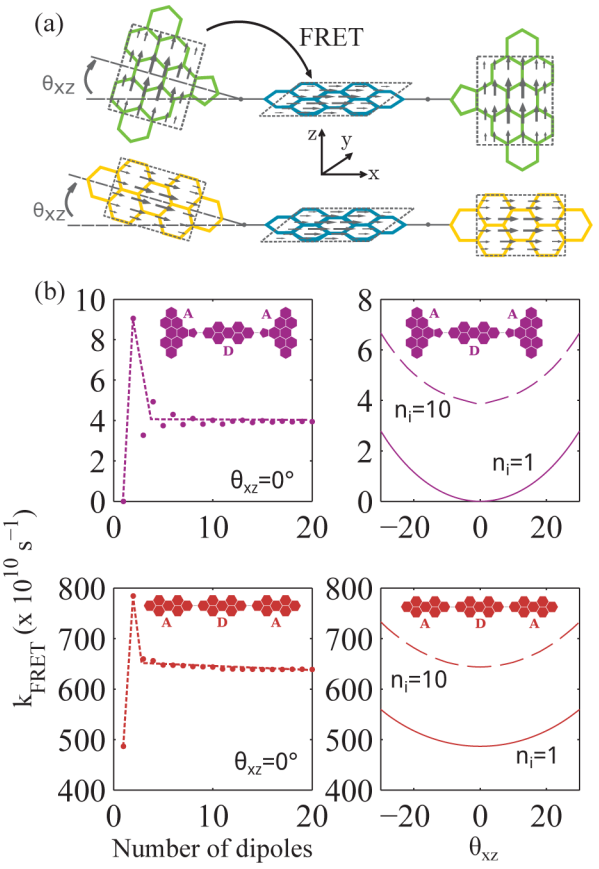

Figure 4. (a) Schematic representation of the FRET model of energy transfer between donor and acceptor in dyes **TH** and **TL**. Dipole transition moments within each chromophore were those from a 2D PIB model, and bending in the D−A bond was introduced by pivoting about the bond midpoint in the x−z plane. (b) Left: the calculated energy transfer rate ($\times 10^{10}$ s^{-1}) as a function of the number of dipoles n_i included along the perylene long-axis, shown for triads **TH** (top) and **TL** (bottom). Right: calculated energy transfer rates as a function of the bending angle θ_{xz} shown in (a) above, plotted for n_i = 1, n_j = 1 (point-dipole model) and n_i = 10, n_j = 7 (line-dipole model). The dashed lines in the left-hand side plots are included as a guide to the eye.

For the linear triad **TL**, the model predicts an energy transfer rate of (0.15 ps)$^{-1}$, which is comparable to the experimentally determined transfer rate of (0.6 ps)$^{-1}$. For the H-shaped triad **TH**, however, the predicted value of (26 ps)$^{-1}$ is more than an order of magnitude slower than the experimental value of (1.2 ps)$^{-1}$. PL anisotropy measurements discussed above indicated that the angle between donor and acceptor transition dipole moments on **TL** (**TH**) may have not be fully aligned (orthogonal). We therefore also explored whether torsions and bending around the N−N bond may have an impact on energy transfer. The energy transfer rate was calculated as a function of the bending angle θ_{xz} of this bond (Figure 4b, right-hand side). Here, the number of elements along the long axis of the perylene units was set to n_i = 10 in order to allow a compromise between the adequate representation of the continuously distributed wave function and the limitations imposed by computational speed. For **TH**, even a relatively large bending angle of 18° between donor and acceptor units only increases the energy transfer rate very slightly up to (21 ps)$^{-1}$, which is still far slower than the experimentally observed value. Therefore, although electronic wave function delocalization and bond bending may account for a large extent of unusually fast energy transfer in the H-shaped triad, a significant discrepancy remains that cannot be accounted for by simple through-space dipole−dipole coupling or by a Frenkel exciton/vibronic model.[22]

We therefore propose that through-bond energy transfer between the strongly electronically coupled donor and acceptor units has a significant contribution to the overall EET in the H-shaped triad. Energy transfer in covalently bound donor−acceptor systems has been studied extensively,[22,25,26,33−42] and both through-space contributions mediated by electronic multipole coupling[25,26] and through-bond mechanisms, which depend on orbital overlap between the two units,[34] have been shown to play a role. For perylene monoimides and bisimides, the location through which donor and acceptor units are linked has a strong impact on the degree of through-bond electronic coupling which can occur.[41,42] When linked through the 9-position of the perylene, extensive conjugation throughout the entire molecule and an absorption spectrum strongly different to those of the constituent chromophores were observed.[41] In contrast, when the PBI unit was linked to the same acceptors through the imide nitrogen, the two units were found to be electronically independent of each other.[42] This difference in behavior has been attributed to the presence of nodes in the frontier molecular orbitals centered on the nitrogen atom in PBI.[43]

The H-shaped triad **TH** investigated here also has donor and acceptor units connected at the imide nitrogens; however, there are several pieces of evidence pointing toward through-bond electronic coupling making a contribution to the unexpectedly rapid energy transfer. First, there is significant deviation between models based on through-space EET and the observed transfer rates. Second, the strong bathochromic shift of the donor S2 ← S0 and acceptor S1 ← S0 transitions of the triad relative to the isolated donor and acceptor dyes, as is evident from absorption and emission spectra (see Figure 1). Third, although the acceptor is linked through the imide nitrogen at the end of the perylene subunit, the donor unit is not. For a coplanar configuaration of the donor and acceptor subunits, therefore, there is extensive delocalization across the entire molecule in several of the orbitals involved in optical transitions (see DFT calculations[44] in the Supporting Information). Direct electronic coupling may therefore be enabled by torsions about the N−N linking bond.[38,45] Hence, a combination of through-space energy transfer facilitated by electronic wave function delocalization, supplemented by through-bond energy transfer, allows an ultrafast energy transfer in **TH** that is accompanied by a switch in polarization.

In conclusion, we have investigated the dynamics of energy transfer and polarization switching for two compound perylene bisimide triad dyes that show excellent potential for use in luminescent solar concentrator devices. For both triad dyes, highly efficient energy transfer from donor to acceptor moieties is shown to occur within less than 2 ps. For the orthogonally arranged H-shaped triad, the observed rates are in sharp contrast with the Förster point-dipole model, which predicts an absence of energy transfer in this geometry. The observed fast rates are shown to arise from a combination of through-space energy transfer between delocalized electronic electronic states, and through-bond energy transfer, mediated by bond-bending and torsions. As a result, a system of two triad dyes is presented that allows for an energy downshift to reduce self-absorption while giving excellent control over emission polarization.

DOI: 10.1021/acs.jpclett.5b00183
J. Phys. Chem. Lett. 2015, 6, 1170−1176

Embedding such triads in a liquid crystal host should result in efficient, switchable LSCs with low self-absorption and surface losses.

■ ASSOCIATED CONTENT

Supporting Information

Materials synthesis and characterization. Experimental details of time-resolved PL. PL quantum efficiencies and PL lifetimes. Time-resolved PL spectrum of acceptor dye. Steady-state PL spectra. Density functional theory. This material is available free of charge via the Internet at http://pubs.acs.org/.

■ AUTHOR INFORMATION

Corresponding Author

*E-mail: l.herz@physics.ox.ac.uk.

Notes

The authors declare no competing financial interest.

■ ACKNOWLEDGMENTS

C.M. thanks the Engineering and Physical Sciences Research Council and Merck Chemicals for financial support through an Industrial CASE studentship. J.t.S. would like to thank Ralf Bovee and Xianwen Lou for their support with the analytical measurements.

■ REFERENCES

(1) Sener, C.; Fthenakis, V. Energy Policy and Financing Options to Achieve Solar Energy Grid Penetration Targets: Accounting for External Costs. *Renewable Sustainable Energy Rev.* **2014**, *32*, 854−868.

(2) Feldman, D.; Barbose, G.; Margolis, R.; Wiser, R.; Darghouth, N.; Goodrich, A. *Photovoltaic (PV) Pricing Trends: Historical, Recent, and Near-Term Projections*, Technical Report DOE/GO-102012-3839; U.S. Department of Energy: Oak Ridge, TN, 2012

(3) Weber, W. H.; Lambe, J. Luminescent Greenhouse Collector for Solar Radiation. *Appl. Opt.* **1976**, *15*, 2299−2300.

(4) Goetzberger, A.; Greube, W. Solar Energy Conversion with Fluorescent Collectors. *Appl. Phys.* **1977**, *14*, 123−139.

(5) Levitt, J. A.; Weber, W. H. Materials for Luminescent Greenhouse Solar Collectors. *Appl. Opt.* **1977**, *16*, 2684−2689.

(6) Batchelder, J. S.; Zewail, A. H.; Cole, T. Luminescent Solar Concentrators. 1: Theory of Operation and Techniques for Performance Evaluation. *Appl. Opt.* **1979**, *18*, 3090−3110.

(7) Debije, M. G.; Verbunt, P. P. C. Thirty Years of Luminescent Solar Concentrator Research: Solar Energy for the Built Environment. *Adv. Energy Mater.* **2012**, *2*, 12−35.

(8) Balaban, B.; Doshay, S.; Osborn, M.; Rodriguez, Y.; Carter, S. A. The Role of FRET in Solar Concentrator Efficiency and Color Tunability. *J. Lumin.* **2014**, *146*, 256−262.

(9) Debije, M. G.; Verbunt, P. P. C.; Rowan, B. C.; Richards, B. S.; Hoeks, T. L. Measured Surface Loss from Luminescent Solar Concentrator Waveguides. *Appl. Opt.* **2008**, *47*, 6763.

(10) McDowall, S.; Johnson, B. L.; Patrick, D. L. Simulations of Luminescent Solar Concentrators: Effects of Polarization and Fluorophore Alignment. *J. Appl. Phys.* **2010**, *108*, 053508.

(11) Verbunt, P. P. C.; Kaiser, A.; Hermans, K.; Bastiaansen, C. W. M.; Broer, D. J.; Debije, M. G. Controlling Light Emission in Luminescent Solar Concentrators through Use of Dye Molecules Aligned in a Planar Manner by Liquid Crystals. *Adv. Funct. Mater.* **2009**, *19*, 2714−2719.

(12) Mulder, C. L.; Reusswig, P. D.; Velázquez, A. M.; Kim, H.; Rotschild, C.; Baldo, M. A. Dye Alignment in Luminescent Solar Concentrators: I. Vertical Alignment for Improved Waveguide Coupling. *Opt. Express* **2010**, *18* (Suppl 1), A79−90.

(13) ter Schiphorst, J.; Kendhale, A. M.; Debije, M. G.; Menelaou, C.; Herz, L. M.; Schenning, A. P. H. J. Dichroic Perylene Bisimide Triad Displaying Energy Transfer in Switchable Luminescent Solar Concentrators. *Chem. Mater.* **2014**, *26*, 3876−3878.

(14) Sadrai, M.; Hadel, L.; Sauers, R. R.; Husain, S.; Krogh-Jespersen, K.; Westbrook, J. D.; Bird, G. R. Lasing Action in a Family of Perylene Derivatives: Singlet Absorption and Emission Spectra, Triplet Absorption and Oxygen Quenching Constants, and Molecular Mechanics and Semiempirical Molecular Orbital Calculations. *J. Phys. Chem.* **1992**, *96*, 7988−7996.

(15) Chen, Z.; Baumeister, U.; Tschierske, C.; Würthner, F. Effect of Core Twisting on Self-Assembly and Optical Properties of Perylene Bisimide Dyes in Solution and Columnar Liquid Crystalline Phases. *Chemistry* **2007**, *13*, 450−65.

(16) Langhals, H.; Hofer, A. Chromophores Arranged as "Magnetic Meta Atoms": Building Blocks for Molecular Metamaterials. *J. Org. Chem.* **2013**, *78*, 5889−97.

(17) Kendhale, A. M.; Schenning, A. P. H. J.; Debije, M. G. Superior Alignment of Multi-Chromophoric Perylenebisimides in Nematic Liquid Crystals and Their Application in Switchable Optical Waveguides. *J. Mater. Chem. A* **2013**, *1*, 229−232.

(18) Debije, M. G.; Menelaou, C.; Herz, L. M.; Schenning, A. P. H. J. Combining Positive and Negative Dichroic Fluorophores for Advanced Light Management in Luminescent Solar Concentrators. *Adv. Opt. Mater.* **2014**, *2*, 687−693.

(19) Dasgupta, D.; Kendhale, A. M.; Debije, M. G.; ter Schiphorst, J.; Shishmanova, I. K.; Portale, G.; Schenning, A. P. H. J. Effect of the Ortho Alkylation of Perylene Bisimides on the Alignment and Self-Assembly Properties. *ChemistryOpen* **2014**, *3*, 138−41.

(20) Adachi, M.; Nagao, Y. Design of near-Infrared Dyes Based on π-Conjugation System Extension 2. Theoretical Elucidation of Framework Extended Derivatives of Perylene Chromophore. *Chem. Mater.* **2001**, *13*, 662−669.

(21) Lakowicz, J. R. *Principles of Fluorescence Spectroscopy*, 3rd ed.; Springer: New York, **2006**; pp 1−954.

(22) Nalbach, P.; Pugliesi, I.; Langhals, H.; Thorwart, M. Noise-Induced Förster Resonant Energy Transfer between Orthogonal Dipoles in Photoexcited Molecules. *Phys. Rev. Lett.* **2012**, *108*, 218302.

(23) Valeur, B.; Berberan-Santos, M. N. *Molecular Fluorescence: Principles and Applications*; John Wiley & Sons: Hoboken, NJ, 2012; p 569.

(24) Parkinson, P.; Kondratuk, D. V.; Menelaou, C.; Gong, J. Q.; Anderson, H. L.; Herz, L. M. Chromophores in Molecular Nanorings: When is a Ring a Ring? *J. Phys. Chem. Lett.* **2014**, *5*, 4356−4361.

(25) Förster, T.; Forster, T. Energiewanderung Und Fluoreszenz. *Die Naturwissenschaften* **1946**, *33*, 166−175.

(26) Förster, T. 10th Spiers Memorial Lecture. Transfer Mechanisms of Electronic Excitation. *Discuss. Faraday Soc.* **1959**, *27*, 7.

(27) Westenhoff, S.; Daniel, C.; Friend, R. H.; Silva, C.; Sundström, V.; Yartsev, A. Exciton Migration in a Polythiophene: Probing the Spatial and Energy Domain by Line-Dipole Forster-Type Energy Transfer. *J. Chem. Phys.* **2005**, *122*, 094903.

(28) Hennebicq, E.; Pourtois, G.; Scholes, G. D.; Herz, L. M.; Russell, D. M.; Silva, C.; Setayesh, S.; Grimsdale, A. C.; Müllen, K.; Brédas, J.-L.; et al. Exciton Migration in Rigid-Rod Conjugated Polymers: An Improved Förster Model. *J. Am. Chem. Soc.* **2005**, *127*, 4744−62.

(29) Krueger, B. P.; Scholes, G. D.; Fleming, G. R. Calculation of Couplings and Energy-Transfer Pathways between the Pigments of LH2 by the Ab Initio Transition Density Cube Method. *J. Phys. Chem. B* **1998**, *102*, 5378−5386.

(30) Lippitz, M.; Hübner, C.; Christ, T.; Eichner, H.; Bordat, P.; Herrmann, A.; Müllen, K.; Basché, T. Coherent Electronic Coupling Versus Localization in Individual Molecular Dimers. *Phys. Rev. Lett.* **2004**, *92*, 103001.

(31) Beenken, W. J. D.; Pullerits, T. Excitonic Coupling in Polythiophenes: Comparison of Different Calculation Methods. *J. Chem. Phys.* **2004**, *120*, 2490−5.

(32) Schmid, S. A.; Abbel, R.; Schenning, A. P. H.; Meijer, E. W.; Sijbesma, R. P.; Herz, L. M. Analyzing the Molecular Weight

DOI: 10.1021/acs.jpclett.5b00183
J. Phys. Chem. Lett. 2015, 6, 1170−1176

Distribution in Supramolecular Polymers. *J. Am. Chem. Soc.* **2009**, *131*, 17696−704.
(33) Kasha, M. Energy Transfer Mechanisms and the Molecular Exciton Model for Molecular Aggregates. *Radiat. Res.* **1963**, *20*, 55.
(34) Dexter, D. L. A Theory of Sensitized Luminescence in Solids. *J. Chem. Phys.* **1953**, *21*, 836.
(35) Lin, S.; Xiao, W.; Dietz, W. Generalized Förster-Dexter Theory of Photoinduced Intramolecular Energy Transfer. *Phys. Rev. E: Stat. Phys., Plasmas, Fluids, Relat. Interdiscip. Top.* **1993**, *47*, 3698−3706.
(36) Scholes, G. D.; Ghiggino, K. P.; Oliver, A. M.; Paddon-Row, M. N. Intramolecular Electronic Energy Transfer between Rigidly Linked Naphthalene and Anthracene Chromophores. *J. Phys. Chem.* **1993**, *97*, 11871−11876.
(37) Speiser, S. Photophysics and Mechanisms of Intramolecular Electronic Energy Transfer in Bichromophoric Molecular Systems: Solution and Supersonic Jet Studies. *Chem. Rev.* **1996**, *96*, 1953−1976.
(38) Holten, D.; Bocian, D. F.; Lindsey, J. S. Probing Electronic Communication in Covalently Linked Multiporphyrin Arrays. A Guide to the Rational Design of Molecular Photonic Devices. *Acc. Chem. Res.* **2002**, *35*, 57−69.
(39) Langhals, H.; Esterbauer, A. J.; Walter, A.; Riedle, E.; Pugliesi, I. Förster Resonant Energy Transfer in Orthogonally Arranged Chromophores. *J. Am. Chem. Soc.* **2010**, *132*, 16777−82.
(40) Schlosser, F.; Sung, J.; Kim, P.; Kim, D.; Würthner, F. Excitation Energy Migration in Covalently Linked Perylene Bisimide Macrocycles. *Chem. Sci.* **2012**, *3*, 2778.
(41) Wang, J.; Yang, E.; Diers, J. R.; Niedzwiedzki, D. M.; Kirmaier, C.; Bocian, D. F.; Lindsey, J. S.; Holten, D. Distinct Photophysical and Electronic Characteristics of Strongly Coupled Dyads Containing a Perylene Accessory Pigment and a Porphyrin, Chlorin, or Bacteriochlorin. *J. Phys. Chem. B* **2013**, *117*, 9288−304.
(42) Yang, E.; Wang, J.; Diers, J. R.; Niedzwiedzki, D. M.; Kirmaier, C.; Bocian, D. F.; Lindsey, J. S.; Holten, D. Probing Electronic Communication for Efficient Light-harvesting Functionality: Dyads Containing a Common Perylene and a Porphyrin, Chlorin, or Bacteriochlorin. *J. Phys. Chem. B* **2014**, *118*, 1630−47.
(43) Langhals, H.; Demmig, S.; Huber, H. Rotational Barriers in Perylene Fluorescent Dyes. *Spectrochim. Acta, Part A* **1988**, *44*, 1189−1193.
(44) Valiev, M.; Bylaska, E.; Govind, N.; Kowalski, K.; Straatsma, T.; Van Dam, H.; Wang, D.; Nieplocha, J.; Apra, E.; Windus, T.; et al. NWChem: A Comprehensive and Scalable Open-source Solution for Large Scale Molecular Simulations. *Comput. Phys. Commun.* **2010**, *181*, 1477−1489.
(45) Hsiao, J.-S.; Krueger, B. P.; Wagner, R. W.; Johnson, T. E.; Delaney, J. K.; Mauzerall, D. C.; Fleming, G. R.; Lindsey, J. S.; Bocian, D. F.; Donohoe, R. J. Soluble Synthetic Multiporphyrin Arrays. 2. Photodynamics of Energy-Transfer Processes. *J. Am. Chem. Soc.* **1996**, *118*, 11181−11193.

DOI: 10.1021/acs.jpclett.5b00183
J. Phys. Chem. Lett. 2015, 6, 1170−1176